RAILWAY BRIDGE MONITORING WITH SAR: A CASE STUDY

Gerardo Di Martino[1], Manuela Esposito[2], Bruna Festa[2], Antonio Iodice[1], Laura Mancini[2], Davod Poreh[1], Daniele Riccio[1], Giuseppe Ruello[1]

[1]DIETI, University of Naples Federico II, Naples, Italy.
[2]DICEA, University of Naples Federico II, Naples, Italy.

ABSTRACT

Spaceborne sensors allow large areas of the Earth to be monitored with small revisit times; conversely, use of in situ techniques frequently limits spatial and/or temporal coverage of critical infrastructure observations. In this paper, some of the potentialities of synthetic aperture radar (SAR) for railway bridge monitoring are explored. The study is focused on a case study regarding a bridge near Triflisco, a small city in Campania, Italy. Twenty-six Cosmo-SkyMed stripmap SAR images were acquired over the area, allowing for a permanent-scatterer (PS) analysis of the bridge structure. Thanks to the availability of a detailed ground truth, the physical nature of the bridge PSs, their spatial distribution, and their time behavior are investigated. In particular, the PS behavior is compared to deformation results obtained using thermal loads in a finite-element model of the bridge.

***Index Terms*—** Synthetic aperture radar, railway bridge, permanent scatterers, F.E.M.

1. INTRODUCTION

Railway infrastructures consist of several different elements spatially distributed over very wide geographical areas. In situ monitoring of all these elements requires the deployment of significant resources in terms of people and/or instrumentation, thus limiting the spatial and/or temporal coverage of the observations. From this viewpoint, remote sensing techniques are particularly appealing, since they allow for frequent monitoring of large areas. In particular, synthetic aperture radar (SAR) is particularly convenient due to its all-weather all-time observation capabilities and to the possibility of estimating centimeter-scale displacements.

In this paper the potentialities of permanent-scatterer (PS) differential interferometry (DInSAR) [1] for the monitoring of deformation parameters of railway bridges are analyzed. In this specific application, it may be of interest to measure the movements of specific objects of small or medium size, so that the PS technique must face limitations that do not emerge in conventional DInSAR processing, where the displacement of spatially distributed areas of the Earth's surface is of interest (e.g., monitoring of subsidence, landslides). The first obvious limitation is that an object can be monitored only if it behaves as a PS; the second is that a PS present in the SAR image cannot be always straightforwardly associated to a specific physical object in the observed scene. Indeed, in scenarios where it is necessary to monitor relative displacements between specific physical structures, it is not sufficient to analyze the average global behavior of PSs present on an extended area, but it is necessary to identify the PSs related to the structures of interest, thus measuring the relative displacement between pairs and/or small groups of PSs.

To overcome these limitations the development of appropriate electromagnetic models is required: these models should allow predicting if a specific object behaves as a PS, assigned the sensor acquisition geometry, the shape and the dimensions of the object and the characteristics of other elements possibly present in the same resolution cell (e.g., vegetation). A meaningful example of this kind of model is presented in [2].

The physical object that gives rise to the PS on the image may be geometrically large and structurally complex, so that its association with the PS (which represents the structure phase center) is usually not straightforward [1]-[4]. In this paper an analysis of PS distribution and behavior over a specific structure, namely the railway bridge near Triflisco, Italy, in order to assess the potentialities of PS DInSAR to perform static monitoring of this kind of infrastructures, is proposed. A priori knowledge of the bridge structure and of its surroundings is exploited to draw significant conclusions on bridge PS characteristics. In particular, a finite-element model (FEM) of the bridge is used and the displacements measured on the PS are compared with those predicted by the FEM using thermal loads.

2. CASE STUDY

The bridge of interest is located in Campania, Italy, close to the small city of Triflisco. Over the area 26 Cosmo-SkyMed stripmap acquisitions are available, spanning the time interval 2011-2015 (see Table I). The images were acquired in descending orbit, HH polarization, with an incidence angle of 26°. In Fig.1 the acquisition geometry is superimposed over a Google Earth image of the bridge. The structure of the bridge can be appreciated from the picture in Fig.2.

TABLE I. LIST OF SAR ACQUISITIONS.

	Year 2011 (6 imgs)		Year 2012 (6 images)		Year 2013 (6 images)		Year 2014 (7 images)		Year 2015 (1 image)
	2011 I Semester (2 images)	2011 II Semester (4 images)	2012 I Semester (3 images)	2012 II Semester (3 images)	2013 I Semester (3 images)	2013 II Semester (3 images)	2014 I Semester (3 images)	2014 II Semester (4 images)	2015 I Semester (1 image)
1	24/02/2011	18/07/2011	11/02/2012	05/08/2012	13/02/2013	23/07/2013	15/01/2014	27/08/2014	23/03/2015
2	29/04/2011	19/08/2011	15/04/2012	08/10/2012	02/04/2013	25/09/2013	05/04/2014	30/10/2014	
3		22/10/2011	18/06/2012	11/12/2012	05/06/2013	28/11/2013	21/04/2014	15/11/2014	
4		25/12/2011						17/12/2014	

Fig.1 SAR acquisition geometry: the line of flight of the sensor is represented in red.

3. BRIDGE PS ANALYSIS

Looking at Fig.2, it is evident that the steel structural elements of the bridge can easily behave as PS, due to their dihedral and trihedral configurations. For this reason, PS DInSAR seems particularly well-suited in this scenario and, therefore, it was applied on the available dataset. A coherence threshold of 0.85 was set for PS selection, thus leading to the identification of fifty PSs associable to the bridge. The detected PSs are shown in Fig.3: note that some of them are very closely spaced, so that they may be undistinguishable. Note also that the non-perfect superposition with the bridge may be due to small geocoding errors.

To support PS analysis a FEM model of the bridge has been developed. The model is outlined in Section 3.1. Two aspects of PS analysis are reported in Sections 3.2 and 3.3.

3.1. F.E.M. Model

To evaluate with precision the effects of the rail-structure interaction, it is necessary to investigate, by non-linear analysis, the thermal load on the bridge, the thermal load on the rail (when expansion devices are provided), and the vertical/longitudinal stresses generated during braking and/or acceleration loads associated with trainsets.

Following in situ surveys, a FEM of the bridge was developed, incorporating accurate structural models of all bridge elements (see Fig.4). The rail-structure interaction models are automatically built by LUSAS starting from geometric properties, material and load characteristics. The

Fig.2 Picture of the bridge.

elaborations performed by the LUSAS software are carried out in compliance with the UIC code (Union Internationale des Chemins de fer) 774-3 [7], which "provides methods for calculating forces and displacements connected to the interaction phenomenon".

Two models have been carried out, due to the lack of reliable data on the pendulum conditions on the Pier 3. Therefore, a model has been obtained with the configuration of the broken pendulum (which became, thus, support) and the other one with the still working pendulum configuration.

Both models were then loaded with thermal loads ΔT, measured at the same time of SAR acquisitions; for each load configuration, both displacements and stress state were evaluated (see Fig.5). The comparison with the output of a dynamic monitoring system allowed to state that the configuration that reflects the current state of the constraint is the one with the pendulum still working.

3.2. PS spatial distribution analysis

Looking at Fig.3 it is noted that PS distribution along the bridge is not uniform: in particular, only few PSs are present at the sides of the bridge. However, due to the regular geometrical structure (see Fig.2), a uniform spatial PS pattern would be expected. Our first goal is to try to justify this phenomenon. Indeed, from the available optical images during the acquisition period the vegetation present on the river bank is not so tall that the bridge structure can be shadowed for the considered incidence angle. However, vegetation is very dense around the bridge, so that it can interfere with PSs according to the phenomenon discussed in [2]. In particular, as shown in [2], the correlation coefficient ρ_{ij} of the generic interferometric pair of acquisitions i and j can be then expressed as

$$|\rho_{ij}| \cong \frac{1}{1+SBR^{-1}} \quad (1)$$

where SBR is the signal-to-background ratio defined as

Fig.3 Green dots represent the PS detected on the bridge.

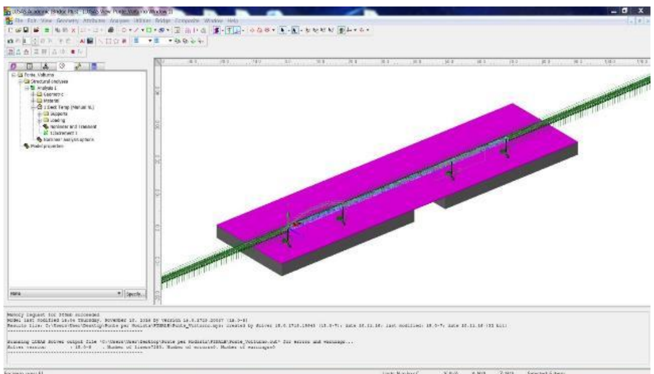
Fig.4 3D model of the bridge used for FEM analysis.

$$SBR = \frac{\sigma_S}{\sigma_D^0 A_r} \tag{2}$$

and σ_S is the PS radar cross section, σ_D is the background normalized radar cross section, and A_r is the resolution cell area. Note that (1) has been obtained in the hypothesis that the correlation coefficient of the distributed background is very small: however, when the background is made up of vegetation or river water, as in our case, this hypothesis can be safely assumed. Indeed, due to layover, the PS related to the bridge structures will be placed in resolution cells with water background in the central part of the bridge and vegetation background at the sides of the bridge. The average SBR for both these situations has been estimated from the images, obtaining 2.78 for PS in vegetation background and 10.71 for PS in river background. Therefore, according to (1) in the former case an average coherence of 0.73 is obtained, whereas in the latter 0.92. Since, the coherence threshold used for PS selection is 0.85, PSs in water background will be selected and those in vegetation background discarded. Few exceptions to this general rule can be appreciated at the right of the bridge in Fig.3, where some PS are selected close to the end of the bridge. These PS are located in the area close to the pillar, where vegetation is probably frequently cut.

3.2. Comparison with FEM analysis

Following PS DInSAR analysis, it was found that in the considered period the bridge was not subject to displacements

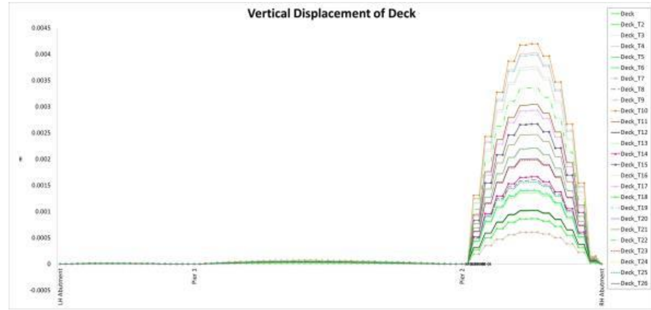

(a)

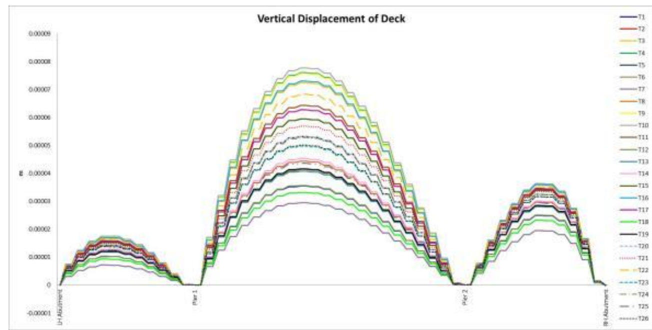

(b)

Fig.5 Vertical displacement of the bridge: (a) Support; (b) Pendulum.

that could be traced back to significant subsidence events. Indeed, a linear trend of the PSs has been observed, but it is related to a speed of the order of fractions of a millimeter per year, i.e. below the accuracy of the technique [5]. However, an oscillating behavior was observed in the estimated dispacements, leading to the conclusion that these displacements could be mainly related to temperature variations, dictating deformation of the materials constituting the bridge [6]. Although the extent of the displacements measured on the PSs, which are in the order of fractions of a millimeter, falls below the sensitivity limit of the PS technique [5], the possibility to extract some useful information is here verified, by comparing the temporal trends of the deformations measured on the PSs and those resulting from the FEM model described in Section 3.1.

In order to procede to the comparison, first of all it was necessary to project the longitudinal (δ_l) and vertical (δ_z) displacements obtained from the FEM in order to obtain line-of-sight displacements (δ_{LOS}). This can be done according to the following relation

$$\delta_{\mathrm{LOS}} = \cos\vartheta * \delta_z + \sin\vartheta * \sin\varphi * \delta_l \tag{3}$$

where $\vartheta = 0.44$ rad is the incidence angle and $\varphi = 0.45$ rad is the angle between bridge direction and sensor line of flight (see Fig.1). After this operation FEM-based displacements are comparable to PS-based ones. In general, the projection along the line of sight of the deformations provided by the FEM model is less than one millimeter; therefore, they are also below the sensitivity of the PS technique. This means, on

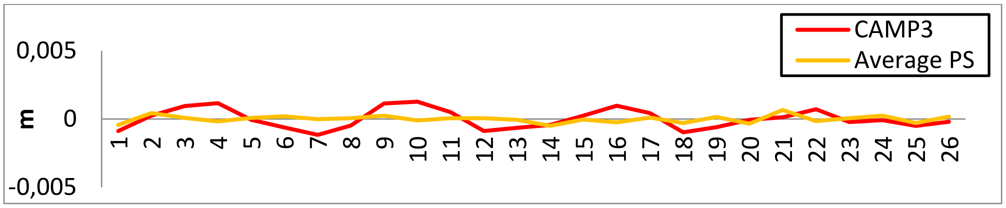

(a)

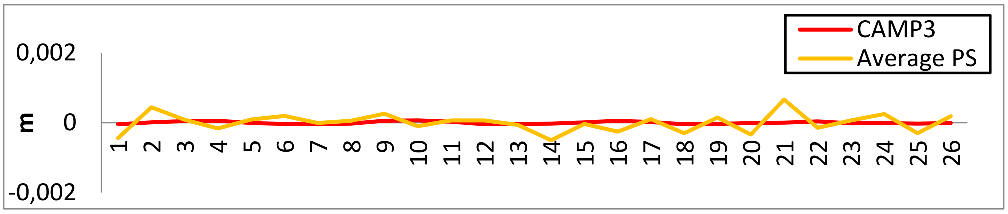

(b)

Fig.6 Comparison between line of sight displacements obtained with FEM (CAMP3) and estimated from PS (Average PS) for span number 3. On the horizontal axis IDs of SAR acquisitions are reported, following chronological order. (a) Support; (b) working pendulum.

the one hand, that the PS technique does not produce "false alarms" in this case, i.e. it does not detect non-existent movements. On the other hand, the PS measures will be mainly linked to spurious effects (atmospheric phase, decorrelation errors). To reduce these effects the PS were divided in groups related to the three different spans of the bridge and the displacements associated to PS of each group were averaged. Even after this operation, no significant correlation was found between FEM and PS displacements, even if the two displacements are in the same range of values.

With regard to the third span of the bridge (northern one), we now focus on the two FEM simulated scenarios, namely support and pendulum. In Fig.6(a) the comparison between PS- and FEM-derived displacements for the third bridge span for the support configuration are shown. It is evident that in this case FEM-derived displacements are significantly larger than PS-based ones. In Fig.6(b) the same comparison for the working-pendulum configuration is reported: in this case the situation is inverted and the displacements of the FEM are smaller than PS ones. In conclusion, PS-based displacements seem to point out an intermediate situation. This allowed us to conclude that the pendulum is still working, even if its functionality is probably gradually degrading.

4. CONCLUSION

In this paper the potentialities of PS as a support for railway bridge monitoring have been discussed. In particular, a case study was presented, relevant to a bridge in Campania, Italy, for which a wide set of information and a set of 26 Cosmo-SkyMed stripmap images were available. A finite element model of the bridge was also developed in order to compare displacements (measured on the PS and obtained through the model). The presented results highlight that for this kind of man-made structures a detailed knowledge of the structure of the bridge and of its surroundings is essential to understand the PS phenomenology.

5. ACKNOWLEDGEMENTS

The Cosmo-SkyMed images were acquired in the frame of the Italian PON Project MODISTA. The authors thank ANSALDO STS for providing the data.

6. REFERENCES

[1] A. Ferretti, C. Prati, F. Rocca, “Permanent scatterers in SAR interferometry”, *IEEE Transactions on Geoscience and Remote Sensing*, Vol. 39, No.1, pp. 8-20, 2001.

[2] G. Di Martino, A. Iodice, D. Poreh, D. Riccio, G. Ruello, “Physical models for evaluating the interferometric coherence of potential persistent scatterers”, *Proceedings of IEEE IGARSS 2017*, Fort Worth (USA), July 2017, pp. 3163-3166.

[3] S. Auer, S. Gernhardt, R. Bamler, “Investigations on the Nature of Persistent Scatterers Based on Simulation Methods”, *Proceedings of the Joint Urban Remote Sensing Event, JURSE 2011,* pp. 61 – 64, Munich (Germany), 2011.

[4] P. Dheenathayalan,D. Small, A. Schubert, and R. F. Hanssen, “High-precision positioning of radar scatterers”, *J. Geod.*, vol. 90, no. 5, pp. 403–422, 2016.

[5] M. Crosetto, O. Monserrat, M. Cuevas-González, N. Devanthéry, and B. Crippa, “Persistent Scatterer Interferometry: A review”, *ISPRS J. Photogramm. Remote Sens.*, vol. 115, pp. 78–89, 2016.

[6] O. Monserrat, M. Crosetto, M. Cuevas, B. Crippa, “The thermal expansion component of Persistent Scatterer Interferometry observations”, *IEEE Geosci. Remote Sens. Lett.*, vol. 8, pp. 864-868, 2011.

[7] UIC 774-3: Track - bridge Interaction. Recommendations for Calculations - Union Internationale des Chemins de fer. October 2001.